

 Open access • Journal Article • DOI:10.1039/B920393A

## **At the interface: solvation and designing ionic liquids** — [Source link](#)

[Robert Hayes](#), [Gregory G. Warr](#), [Rob Atkin](#)

**Institutions:** [University of Newcastle](#), [University of Sydney](#)

**Published on:** 09 Feb 2010 - [Physical Chemistry Chemical Physics](#) (Royal Society of Chemistry)

**Topics:** [Ionic liquid](#)

Related papers:

- [Structure in Confined Room-Temperature Ionic Liquids](#)
- [Molecular layering of fluorinated ionic liquids at a charged sapphire \(0001\) surface.](#)
- [Double Layer Structure of Ionic Liquids at the Au\(111\) Electrode Interface: An Atomic Force Microscopy Investigation](#)
- [Ionic-liquid materials for the electrochemical challenges of the future.](#)
- [Layering and shear properties of an ionic liquid, 1-ethyl-3-methylimidazolium ethylsulfate, confined to nano-films between mica surfaces](#)

Share this paper:    

View more about this paper here: <https://typeset.io/papers/at-the-interface-solvation-and-designing-ionic-liquids-2v1tcsjpgf>



NOVA

University of Newcastle Research Online

nova.newcastle.edu.au

Hayes RL, Warr GG, Atkin R, 'At the interface: Solvation and designing ionic liquids'.  
Originally published in Physical Chemistry Chemical Physics, 12 1709-1723 (2010)

Available from: <http://dx.doi.org/10.1039/b920393a>

Accessed from: <http://hdl.handle.net/1959.13/930298>

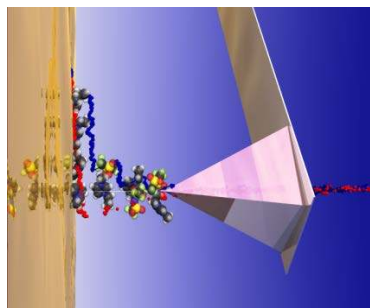
# At the Interface: Solvation and Designing Ionic Liquids

Robert Hayes,<sup>1</sup> Gregory G. Warr<sup>2</sup> and Rob Atkin<sup>1\*</sup>

<sup>1</sup> *Centre for Organic Electronics, Chemistry Building, The University of Newcastle, Callaghan, NSW 2308, Australia*

<sup>2</sup> *School of Chemistry, The University of Sydney, NSW 2006, Australia*

## Graphical Contents Entry



Recent experiments, which show interfacial IL nanostructure is a consequence of both surface specific and bulk liquid interactions, enable us to develop molecular design rules for controlling interfacial IL behavior.

## Abstract

Ionic Liquids' (ILs) remarkable and tunable physicochemical properties mean they have distinct performance advantages over conventional solvents in many settings. However, the use of ILs in surface dependent processes (e.g. electrodeposition, heterogeneous catalysis, dye solar cells) is hindered by the lack of a systematic understanding of IL interfacial structure. In this Perspective Review, we highlight recent experiments which show interfacial IL nanostructure is a consequence of both surface specific and bulk liquid interactions. These results enable us to develop molecular design rules for controlling interfacial IL behavior.

---

\* To whom correspondence should be addressed: [Rob.Atkin@newcastle.edu.au](mailto:Rob.Atkin@newcastle.edu.au)

## 1. Introduction

Within the rich landscape of chemical solvents,<sup>[1]</sup> ionic liquids (ILs) occupy a unique and fascinating position. As salts composed solely of ions, one might reasonably expect ILs to be crystalline solids at ambient temperatures due to electrostatic forces.<sup>[2]</sup> However, by incorporating sterically-mismatched anions and cations, ILs melt below 100°C because, compared to common inorganic salts, Coulombic attractions are dampened and lattice-packing arrangements frustrated.<sup>[3]</sup>

ILs reside at the intersection between solution and materials chemistry and as such their history reflects progress in both disciplines.<sup>[4]</sup> Their journey from niche electrolytes<sup>[5]</sup> to mainstream appeal<sup>[6-9]</sup> has been driven by green principles<sup>[10-12]</sup> and often remarkable physicochemical properties.<sup>[6,13-16]</sup> These features, combined with the relative ease in which they can be prepared, handled and even distilled<sup>[15,17,18]</sup> under standard laboratory conditions, has even inspired several authors to advocate ILs as wholesale replacements for conventional solvents.<sup>[19-21]</sup>

Although first reported in 1914,<sup>[22]</sup> perceptions as to what constitutes an IL are still evolving.<sup>[23]</sup> Suggestions vary from condensed (ionic crystal and liquid) phases of matter<sup>[24,25]</sup> to fragile glass-forming systems<sup>[26,27]</sup> or the missing link between aqueous/organic solutions and high-temperature molten salts.<sup>[28]</sup> Others have drawn analogies to solvent mixtures,<sup>[29]</sup> whereby the anions and cations<sup>[23]</sup> or ionic and non-ionic<sup>[30]</sup> segments are seen as discrete components in the liquid phase. The vast number of potential ILs<sup>[11]</sup> complicates this discussion, as a diverse range of liquid chemistries are possible.

ILs can be defined as protic or aprotic, depending on the mechanism of cation formation.<sup>[13,31]</sup> Other categories, notably the chiral subset,<sup>[32,33]</sup> may include both protic and aprotic ILs. Protic ILs are formed by a proton transfer reaction between an acid and base, which means they donate

and accept hydrogen bonds, assembling H-bonded networks physically and chemically reminiscent of water.<sup>[15,34-37]</sup> This proton transfer is a chemical equilibrium, and MacFarlane & Seddon argue that the resulting fluid should only be considered a pure “ionic liquid” if the concentration of neutral species is less than 1%.<sup>[38]</sup> Alternatively, Angell & co-workers<sup>[18]</sup> defined “strong” and “weak” ILs from comparisons with well-understood ideal aqueous behavior using Walden plots of molar conductivity versus fluidity.

Charge-transfer metathesis and quaternization reactions produce aprotic ILs, often consisting of organic imidazolium or pyrrolidinium-based cations. Aprotic ILs form inter- and intra-molecular hydrogen bonds, but usually not networks like protics. IL synthesis is discussed in detail in the comprehensive reviews by Davis *et. al.*<sup>[39]</sup> and Beyersdorff *et. al.*<sup>[40]</sup>

The emergence of ILs as solvents has instigated several new and exciting areas of scientific research. Since the discovery that ILs could be made with air- and water-stable anions,<sup>[41,42]</sup> ILs have been used in a host of chemical applications including organic synthesis,<sup>[8,43]</sup> catalysis,<sup>[8,44]</sup> electrodeposition,<sup>[28,45,46]</sup> dye-sensitized solar cells<sup>[47]</sup> and lubrication,<sup>[48]</sup> *inter alia*. Moreover, there appears to be certain synergism between ILs and nanotechnology, as various products of the nanotechnology revolution (polymers,<sup>[49-51]</sup> nanoparticles,<sup>[52-55]</sup> nanotubes,<sup>[56,57]</sup> microemulsions<sup>[58-60]</sup>) have conspicuously well-regulated nanoscopic structure when prepared in ILs. This is not a coincidence. Mounting experimental<sup>[61-68]</sup> and theoretical<sup>[69-72]</sup> evidence suggests ILs are heterogeneous on the nanoscale, with polar and apolar domains in the bulk liquid. In some respects, this model is structurally analogous to a thermodynamically stable bicontinuous microemulsion, but with length scales at least an order of magnitude lower. A structured liquid morphology accounts for IL’s ability to dissolve unusual combinations of solutes, and provides insight into some distinct performance advantages over molecular solvents.

Much current IL research focuses on their ‘designer’ characteristics,<sup>[7]</sup> namely, the capacity to tune key intermolecular forces that govern liquid behaviour. IL structure-property relationships arise from a delicate balance of long-range (Coulombic) and short-range (van der Waals, dipole-dipole, hydrogen bonding, solvophobic<sup>[73]</sup>) interactions, programmed by the choice of anions and cations. Thus, as summarized in Figure 1, *molecular control* of liquid properties is possible depending on how the ions are functionalized.<sup>[7,74]</sup> Unlike conventional solvents, this enables important solvency parameters (polarity, viscosity, cohesive energy, etc.) to be changed at the chemist’s discretion, as molecular structure determines the set of intermolecular forces expressed.<sup>[75,76]</sup> IL solvents can therefore be designed for a particular reaction or process similar to retrosynthetic methodologies in organic chemistry<sup>[77,7]</sup> a significant departure from empirical approaches to solvent selection; Desirable physicochemical properties can be identified from which to work backwards to determine appropriate IL molecular structures.

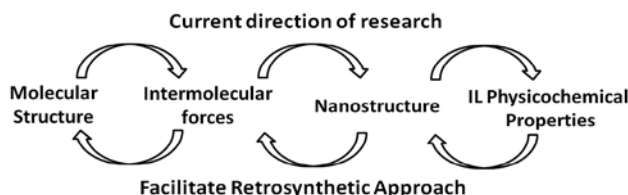


**Figure 1.** Schematic representation of the current scientific paradigm in IL research. This simplified diagram is analogous to retrosynthetic methodologies in organic chemistry.

Compared to bulk liquid structure, the arrangement of IL ions at solid-liquid interface has received scant attention, and yet many promising IL-based applications involve interfaces. One reason the chemical and economic potential of ILs remains unfulfilled is that design rules for controlling interfacial behaviour are only beginning to be determined.<sup>[67,78-82]</sup> Sum frequency

generation (SFG) spectroscopy has revealed the orientation of the first ion layer adjacent to solid (silica,<sup>[88,89]</sup> quartz,<sup>[90,91]</sup> Pt,<sup>[92-95]</sup> TiO<sub>2</sub><sup>[96]</sup>) or air<sup>[97-101]</sup> interfaces. To probe whether order is present beyond this first layer, X-ray<sup>[102-105]</sup> and neutron reflectivity,<sup>[106]</sup> and computer simulations<sup>[57,107-112]</sup> have been employed. These studies suggest an oscillatory ion density profile at the interface, similar to reports of solvation layers in molecular liquids.<sup>[83]</sup> The period of the oscillations is consistent predicted (anion + cation) dimensions, and the distance the distance the interfacial structure propagates into the bulk liquid depends on the structure of the ions. Despite this progress, the strength of IL-substrate interactions, and of cohesive interactions within layers, has not been revealed. Equally, the orientation of ions within the near surface layers elucidated. In conventional molecular solvents interfacial forces are controlled using amphiphilic compounds.<sup>[83-85]</sup> Amphiphiles can serve the same purpose in ILs,<sup>[86,87]</sup> however in some cases the IL itself (usually the cation) is surface active. The ability to fix a robust interfacial nanostructure that can endure static and dynamic operating conditions is attractive, especially for situations where surfactant or polymer adsorption is undesirable.

In this Perspective Review, we highlight recent research into interfacial IL nanostructure, which is shown to be a consequence of surface specific and ‘solvophobic’<sup>[73]</sup> interactions.

Solvophobicity in a non-aqueous solvent is analogous to the ‘hydrophobic effect’<sup>[113]</sup> in water, and is central to IL molecular organization in the bulk and within solvation layers at solid interfaces. The overarching consequence of solvophobic forces is that the bulk and surface structures are closely related. This finding allows us to make inferences for molecularly designing ILs likely to be suitable for a given application, depending on whether near-surface order is desirable or not.

## 2. Solvation Layers in Molecular Liquids

Close to an interface, the molecular organization of fluids is often different to that in the bulk.<sup>[83,114]</sup> Within the solvation zone immediately adjacent to a flat solid, mobile liquid molecules are induced into discrete layers. This liquid ordering, termed ‘solvation layers,’ is characterized by an oscillatory molecular density profile that extends a few molecular diameters from the interface. The associated ‘solvation force’ cannot be explained by continuum theories of van der Waals, or electrostatic forces<sup>[114-116]</sup> as it is mainly of geometric origin, and even occurs in the absence of attractive surface-liquid interactions.<sup>[83]</sup>

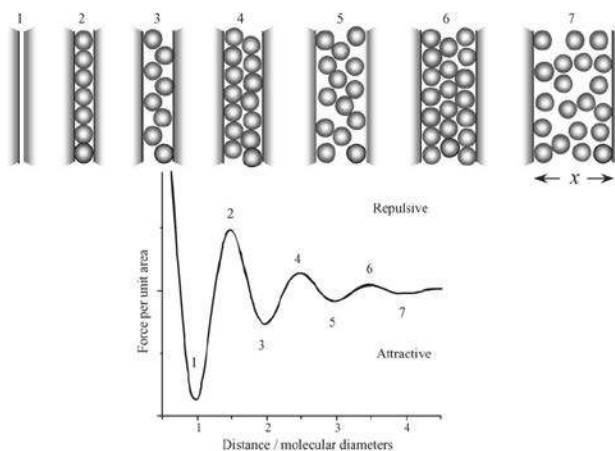
Theoretical descriptions of solvation layers first appeared in the literature in the 1970s. Both Monte Carlo simulations<sup>[117-121]</sup> and formalist hypernetted-chain approximations<sup>[122]</sup> suggested spherical liquid molecules had oscillatory molecular density profiles when confined between two hard walls. In 1981, Horn & Isrealachvili offered the first experimental evidence of solvation layers using the newly developed surface forces apparatus (SFA).<sup>[123]</sup> They measured oscillatory forces for octamethylcyclotetrasiloxane (OMCTS) confined between atomically smooth mica surfaces as a function of absolute separation, confirming alternating regions of attraction and repulsion. The period of oscillation corresponded to the size of the solvent molecules whilst the amplitude decreased with increasing separation. The form of the data was consistent with layers of OMCTS being squeezed out of the closing gap (c.f. Figure 2).<sup>[87]</sup>

Further experiments with other liquids revealed that the number of oscillations decreased with increasing molecular flexibility, as flexible molecules can pack (space fill) effectively without layering.<sup>[124]</sup> Surface roughness of the order of the size of the solvent molecule, was shown to disrupt layering, so that oscillations were smeared out and replaced by a purely monotonic force that still originates from discrete molecular structure.<sup>[83,123]</sup> Hydrogen bonding<sup>[125]</sup> or temperature



changes, such as supercooling the solvent to below its freezing point,<sup>[126]</sup> had negligible effects on the solvation force. This latter finding means that solvation layering in molecular liquids is not a consequence of surface-mediated ‘pre-freezing’ of the liquid.<sup>[83]</sup>

The invention of the Atomic Force Microscope (AFM) has allowed near-surface molecular ordering to be studied on a much wider variety of substrates.<sup>[127-132]</sup> Initially developed to image the topography of insulating surfaces with a sharp tip,<sup>[133]</sup> AFM has become a standard tool in physical chemistry for high resolution surface force measurements.<sup>[114,134]</sup> Force-resolution is sensitive to the AFM tip geometry,<sup>[135,136]</sup> spring constant<sup>[137]</sup> and apparent roughness.<sup>[136]</sup> Within a specially designed fluid cell,<sup>[138]</sup> the AFM allows the structure and composition of interfacial layers to be determined, as well as the interaction strength between the surface and adjacent liquid molecules. Compared to SFA, AFM has smaller ( $\sim \times 10^6$ ) and less well-defined contact area, and the absolute separation between tip and surface is unknown.

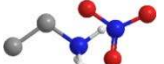
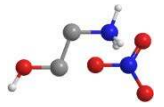
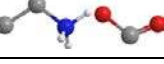
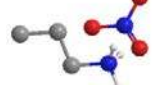
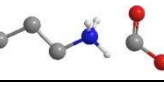
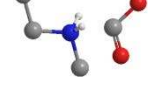


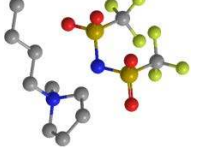
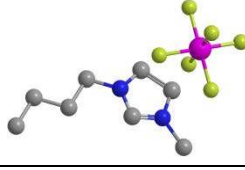
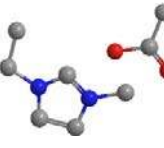


**Figure 2.** Schematic structure of a simple liquid confined between two parallel walls. The order changes drastically depending on distance, which results in an oscillatory force.<sup>†</sup>

<sup>†</sup> Reprinted from Surface Science Reports, 59(1-6); H.-J. Butt, B. Cappella, M. Kappl; Force measurements with the atomic force microscope: Technique, interpretation and applications, p. 1-152, 2005 with permission from Elsevier

In recent years, computer models have been used to simulate solvation forces acting in molecular liquids confined between an AFM tip and solid surface. The tip and substrate are represented as large and infinitely large spherical bodies respectively<sup>[139,140]</sup> or rigid arrays of atoms<sup>[141]</sup> in the vicinity of interacting fluid particles. Whilst direct comparison with experimental results is limited (the models do not account for dispersion forces associated with tip-substrate interactions), the findings are qualitatively similar and show that the liquid particles in the solvation zone are highly ordered compared to the bulk. Increasing the radius of the AFM tip was found to affect the amplitude of the theoretical force oscillations but not the step sizes.

**Table 1.** Structure, molecular weight (MW), density ( $\rho$ ), molecular volume ( $M_v$ ), ion pair diameter ( $D_m$ ), melting point (MP) and H<sub>2</sub>O content of the ionic liquids examined.  $M_v$  is determined from  $\rho$  and MW while  $D_m$  is found by taking the cube root of  $M_v$  as described by Horn et al.,<sup>[142]</sup> which assumes a cubic packing geometry. Carbon atoms are shaded grey, nitrogen are blue, fluorine are yellow, sulfur are orange, phosphorus are pink, oxygen are red. Only polar hydrogens (in white) are shown.

IL	Structure	MW (g.mol <sup>-1</sup> )	$\rho$ (g.cm <sup>-3</sup> )	$M_v$ (nm <sup>3</sup> )	$D_m$ (nm)	MP (°C)	H <sub>2</sub> O content
Ethylammonium Nitrate (EAN)		108.1	1.21	0.15	0.53	13	<0.01 v/v%
Ethanolammonium Nitrate (EtAN)		124.0	1.26	0.16	0.54	-25.2	<0.01 v/v%
Ethylammonium Formate (EAF)		91.1	0.99	0.15	0.53	-15	0.5wt%
Propylammonium Nitrate (PAN)		122.1	1.16	0.18	0.56	3.5	<0.01 v/v%
Propylammonium Formate (PAF)		105.1	0.90	0.19	0.57	-55.4	0.5wt%
Ethylmethylammonium formate (EMAF)		106.1	1.03	0.17	0.56	-	0.5wt%
Dimethylethylammonium formate (DMEAF)		119.2	1.03	0.19	0.57	-	0.5wt%
1-ethyl-3-methylimidazolium bis(trifluoromethane sulfonyl) imide ([EMIm]TFSA)		391	1.51	0.43	0.75	-15	2ppm
1-butyl-1-methylpyrrolidinium bis(trifluoromethane sulfonyl) imide ([BMP]TFSA)		422	1.41	0.50	0.79	-6	2ppm
1-butyl-3-methyl-imidazolium hexafluorophosphate ([BMIm]PF <sub>6</sub> )		284	1.37	0.34	0.70	12	< 0.1 v/v%
1-ethyl-3-methylimidazolium acetate ([EMIm]Ac)		170	1.03	0.27	0.65	< -20	0.35 v/v%

### 3. Solvation Layers in Ionic Liquids

In this section the structure of ILs at mica, silica, graphite and gold interfaces is reviewed. The EAN – mica and PAN – mica systems are considered first, as both the structure of the bulk liquids<sup>[62,63,67]</sup> and the surface properties<sup>[78,142]</sup> are well defined. In the context of solvation layer formation it is important to realize that EAN and PAN, composed only of an ethyl or propyl chains and a charged ammonium headgroup, respond to the solvophobic effect and are induced into disordered sponge-like phases reminiscent of traditional surfactant self-assembly.<sup>[62,63,67]</sup> Thus, when these same ILs are observed under confinement, a basis for liquid ordering is already present; open to question is how the solid surface effects this structure. These results provide a framework for interpreting force experiments on mica for other protic and aprotic ILs, for which the bulk IL structure is not known in most cases. Data obtained using silica, graphite and gold substrates is then described. Silica is rougher and has lower surface charge density than mica, which reduces the level of interfacial order. Graphite is atomically smooth, but interacts solvophobically with the ionic liquid rather than electrostatically, which alters the interfacial structure. The gold (111) surfaces examined are atomically smooth but have lower surface charge than mica, which produces subtle variation in the force data.

#### 3.1 Mica

##### *Protic ILs on Mica*

Not long after the earliest investigations of solvation layers in molecular liquids, Horn *et al.* detected oscillatory force profiles in an IL<sup>‡</sup> using SFA.<sup>[142]</sup> Four to five oscillations were

---

<sup>‡</sup> The paper refers to the IL as a ‘molten salt at room temperature.’

measured for the protic IL ethylammonium nitrate (EAN) before the repulsion became so strong that it prevented closer approach of the mica surfaces. The step period of 0.5-0.6 nm was consistent with the size of the EAN ion pair assuming a cubic packing geometry, suggesting the cation and anion are present in approximately equal numbers in the layers. The force required to squeeze-out a layer decreased farther from the surface as the level of liquid ordering lowered. The authors inferred that up to nine layers were present on the basis of absolute mica-mica separations. Moreover, the similarity of the data to other nonpolar solvents suggested that neither the ionic nature of EAN nor its capacity to form a hydrogen-bonding network significantly affected solvation layer formation. However, as water was added, the electrical double layer force began to dominate, and at 50:50 (v/v%) EAN:H<sub>2</sub>O, the solution behaved as a typical 1:1 electrolyte.

A quarter of a century later, surface structuring was revisited for both protic and aprotic ILs confined between Si<sub>3</sub>N<sub>4</sub> AFM tips, and solid substrates.<sup>[78-82]</sup> Two main features are consistently seen in the AFM data: (1) a series of repeating ‘push-throughs’ at discrete separations on tip approach and (sometimes) retraction and (2) a significant increase in the rupture force closer to the surface. Both of these results are indicative of near-surface liquid ordering that is more pronounced closer to the substrate. The contrast between the oscillatory results obtained by Horn *et. al.* and the stepwise AFM data can be ascribed to the differences in the experimental methods. Typical AFM force versus separation data for the EAN - mica system is shown in Figure 3A and may be rationalized as follows. At tip-surface distances greater than 4 nm, zero force is recorded as the tip experiences negligible resistance as it moves through the IL towards the mica. This point is significant, as it shows that the AFM is insensitive to the relatively disordered structure that exists in the bulk EAN.<sup>[62,63,67]</sup> At 4.1 nm the tip encounters the first detectable solvation

layer and pushes against it. The force increases up to 0.1 nN then the tip ruptures the layer and ‘jumps’ 0.5 nm before it encounters another layer 3.6 nm from the interface, and the process is repeated. The jump interval in all cases is 0.5 nm, in excellent agreement with the predicted ion pair diameter of EAN (Table 1) and previous SFA results.<sup>[142]</sup> Solvation forces increase sharply close to the substrate: the rupture force for the 6<sup>th</sup> solvation layer is only a fifth of that of the layer nearest the substrate, showing the layers closest to the surface are most organized. Attractions between adsorbed EA<sup>+</sup> cations on the tip and substrate are responsible for the adhesion force (6 nN) upon retraction. Zero force is reached at a separation of 2 nm, which corresponds to the fourth measured solvent layer.

In isolation, force measurements cannot determine whether there is a preferred orientation within the layers of ion pairs. However, the fact that EAN is autophobic on mica<sup>[142]</sup> suggests that EA<sup>+</sup> cations are adsorbed first; ammonium headgroup associated with the negatively charged surface and ethyl groups pointing out to the bulk. This hypothesis should lead to a thinner innermost layer on mica composed mostly of cations, however from Figure 3A, the thickness of the step closest to the substrate remains the same as subsequent steps. As one EA<sup>+</sup> occupies an area greater than the size of a mica charge site (one per 0.48 nm<sup>2</sup>),<sup>[143]</sup> even at cation saturation coverage, the degree of substrate charge quenching cannot exceed 87%.<sup>[142]</sup> Thus, we contend that an electrostatically bound layer of cations is present at the interface which the tip cannot penetrate. This means the ‘zero’ distance on the force profile in fact corresponds to a strongly-bound, compact cation layer. The first non-adsorbed layer detected by AFM is then likely to consist of an EAN ion pair; the EA<sup>+</sup> cations arranged nearest to the substrate and oriented with alkyl groups pointing towards the surface to maximise solvophobic interactions with surface

bound cations. This is followed by a  $\text{NO}_3^-$  anion layer above the  $\text{EA}^+$  ammonium headgroup, to quench the electrostatic charge.

In molecular liquids, small changes in temperature have no significant effect on solvation layering.<sup>[83,126]</sup> While this holds for the *bulk* structure of ILs,<sup>[67]</sup> force versus distance curves for the EAN-mica system (Figure 3B) show a significant temperature dependence.<sup>[79]</sup> As the temperature is increased from 14 °C to 30 °C the number of layers present decreases from 7 to 4 layers. The force required to rupture the innermost solvation layer also decreases by more than half. Both results are due to increased thermal motion of ions, disrupting solvophobic attractions between cation alkyl groups which decreases liquid structuring. In each instance the step size remains unchanged at 0.5 nm, consistent with EAN's constant density over this temperature range.

Increasing the length of the cation alkyl group from ethyl to propyl notably changes the force profile (Figure 3C).<sup>[78]</sup> The propyl group confers more rotational freedom than an ethyl group and hence can pack efficiently without layering. As a result fewer layers are detected, and those that are present are no longer vertical, reminiscent of SFA results in molecular liquids that compared the interfacial behaviour of flexible n-octane to inflexible cyclohexane.<sup>[124]</sup> Critically, the innermost layer at 0.5 nm was not always present in PAN, and the expected third step at 1.5 nm was rarely observed. The adhesion observed on retraction is greater for PAN than for EAN, due to stronger solvophobic interactions between propyl moieties of  $\text{PA}^+$  ions adsorbed to mica and the tip.

Covalent tethering of an hydroxyl moiety to the ethyl chain in ethanolammonium nitrate (EtAN) dramatically alters the form of the approach data (Figure 3D).<sup>[79,81]</sup> EtAN exhibits fewer surface layers than either EAN or PAN. This might reasonably be expected, as the melting point of

EtAN is 38°C below that of EAN (Table 1), and the results for EAN demonstrate that layering decreases the further the temperature is increased above melting point. Further, the measured steps for EtAN are non-vertical. This indicates that EtAN is much less ordered near the surface, with the compressibility of EtAN layers attributed to the greater flexibility of the longer cation chain, similar to arguments made for PAN.

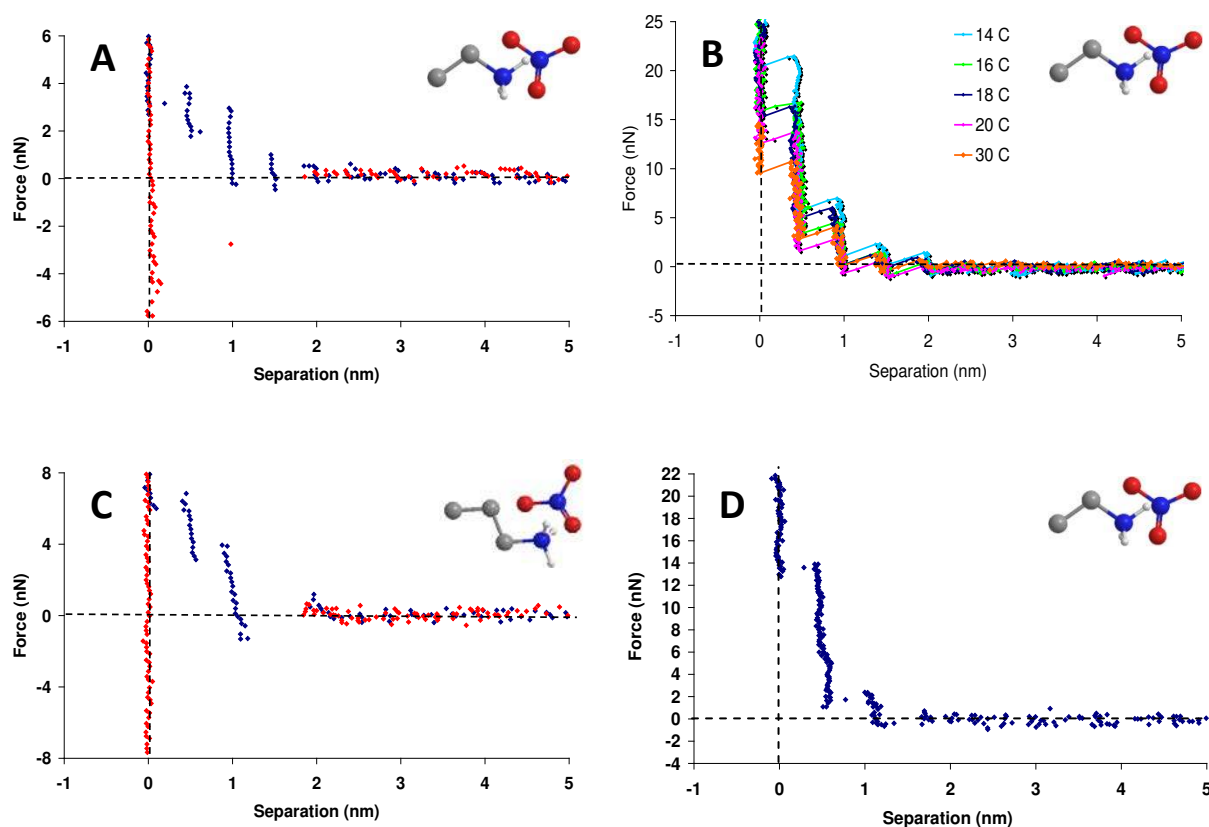


**Figure 3.** Force versus distance profile for an AFM tip approaching (blue) and retracting from (red) a mica surface in various protic ILs (A) EAN at 21°C (Reproduced with permission from Reference [73]) (B) EAN at various temperatures. The forces here are directly comparable as the same  $\text{Si}_3\text{N}_4$  tip was used in all temperature experiments. (C) PAN at 21°C. (Reproduced with permission from Reference [73]) (D) EtAN at 21°C. (Reproduced with permission from Reference [74]).



Fewer layers are detected when the nitrate anion is replaced with a formate anion (EAF and PAF), c.f. Figure 4A and 4B. As with EtAN, this might be expected from the melting points of EAF and PAF, which are 28°C and 64°C lower than those of EAN and PAN, respectively (see Table 1). Like the corresponding nitrates, the retraction curves for EAF and PAF show a strong adhesion between the cation layers adsorbed to the AFM tip and the mica substrate, requiring a force in excess of 10 nN to withdraw the tip; interactions between ethylammonium ions and both the AFM tip and mica substrate seem to be unaffected by changing anion.

Of particular interest is the force profile of PAF in Figure 4B, where the ion pairs are so weakly bound together that the AFM tip is able to disrupt one ion sub-layer and leave the other intact. This provides the clearest proof of alternating interfacial sublayers of cations and anions in ILs. Significantly thinner than expected steps are observed at 0.28, 0.60 nm, 0.83 and 1.17 nm. As zero separation corresponds to a layer of  $\text{PA}^+$  ions electrostatically adsorbed to mica with the propyl chains oriented towards the bulk, we postulate that the closest measurable layer at 0.28 nm corresponds to second  $\text{PA}^+$  layer with alkyl tails orientated towards the mica surface, interacting solvophobically with adsorbed cations. The distinct step between 0.28 and 0.60 nm therefore equates to a neutralising layer of  $\text{HCOO}^-$  anions. The proposed thickness of the cation sub-layer is 0.28 nm and the anion sub-layer of 0.32 nm, yielding a total thickness of 0.6 nm consistent with the ion pair diameter of PAF. The next two layers have similar thicknesses within the accuracy of the measurement. It should be noted cation and anion separation was sometimes observed for EAF, but not consistently enough to be related in detail.

The secondary and tertiary ammonium salts (Figures 4C & D)<sup>[79]</sup> ethylmethylammonium formate (EMAF) and dimethylethylammonium formate (DMEAF) only exhibit single layers at a separation of 0.57 nm and 0.45 nm thick respectively, with relatively small (2nN) and large

rupture forces (8 nN).<sup>§</sup> The spacing measured in EMAF is in good agreement with the calculated ion pair diameter (Table 1) and it is expected that one (cation + anion) solvation layer is present in addition to a surface adsorbed layer of cations that, like EAN, the tip cannot penetrate.

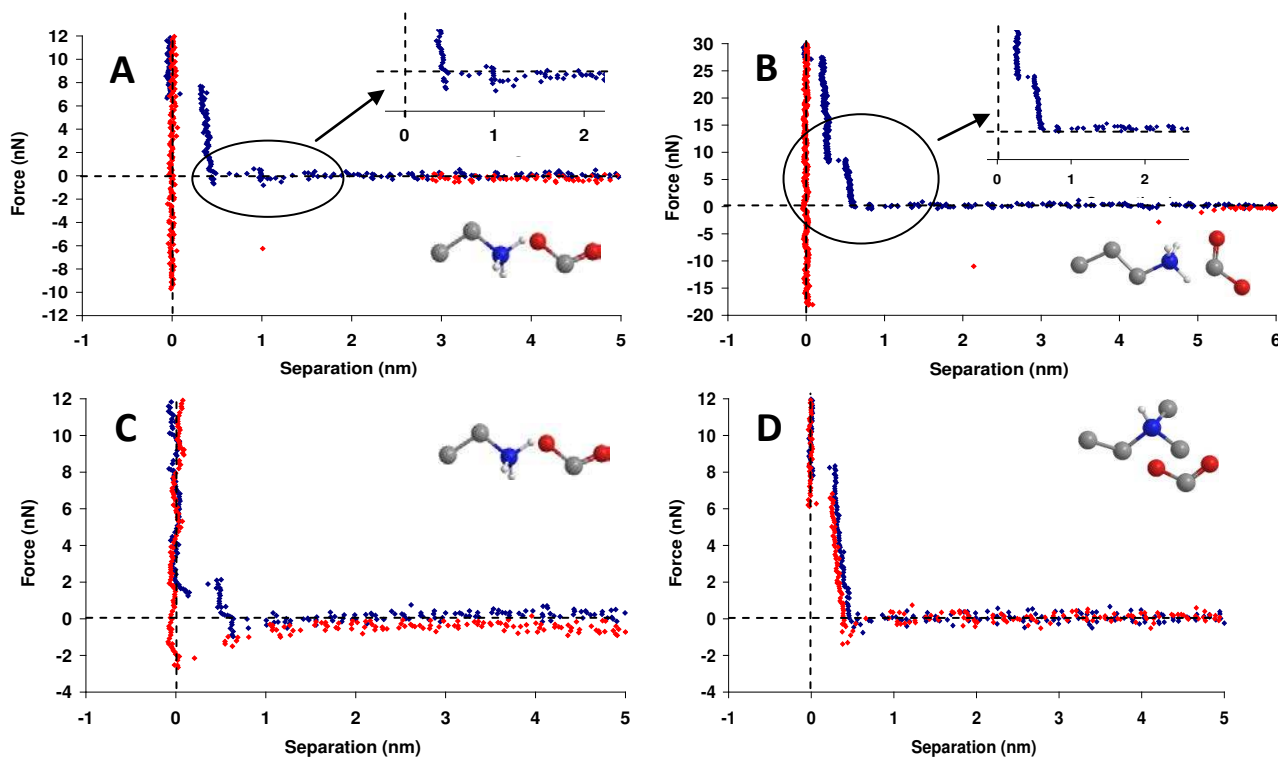


**Figure 4.** Force versus distance profile for an AFM tip approaching (blue) and retracting from (red) a mica surface at 21°C in (A) EAF, (B) PAF, (C) EMAF and (D) DMEAF (Reproduced with permission from Reference [74]).

The measured step size for DMEAF is conspicuously thin, 21% smaller than predicted from ion pair geometry. This provides strong evidence for a layer of weakly surface-adsorbed cations with no solvation layers reaching further into solution. Steric-hindrance of the DMEA<sup>+</sup> charge centre prevents close approach to the substrate, reducing the strength of electrostatic attractions to the mica binding site, and allowing the AFM tip to displace the cation layer and move into contact

<sup>§</sup> The formate based alkylammonium protic ILs are examined as the corresponding nitrates are explosive at room temperature!

with the surface. Unlike the primary and secondary ammonium cations, no strong adhesion is observed on retraction, consistent with the direct tip-mica contact.

### *Aprotic ILs on Mica*

The force profiles for the aprotic ILs 1-ethyl-3-methylimidazolium bis(trifluoromethane sulfonyl) imide (EMIm TFSA) and 1-butyl-1-methylpyrrolidinium bis(trifluoromethane sulfonyl) imide (BMP TFSA) are shown in Figure 5A and 5B.<sup>[80]</sup> The step width in all cases is in excellent agreement with the predicted ion pair diameters (Table 1) and Bragg spacings from prior crystallographic data.<sup>[144]</sup> Solvation forces increase sharply close to the substrate, indicating robust liquid interfacial structure near the surface. Upon tip retraction (shown in red) the force varies in a similar step-wise fashion due to spontaneous reformation of liquid layers.

Solvophobic attractions between the alkyl groups of cations adsorbed to the AFM tip and cations present adsorbed to the substrate or within layers are responsible for the small adhesive forces.

In comparison to other ILs reported in this series of experiments, the interfacial ordering of 1-butyl-3-methyl-imidazolium hexafluorophosphate [BMIm]PF<sub>6</sub> (Figure 5D), is particularly pronounced. Six solvation layers are detected on approach and almost as many upon retraction.<sup>[80]</sup> The non-vertical ‘push-throughs’ are due to molecular flexibility imparted by the imidazolium butyl moiety, as per PAN argument developed above. The high number of layers detected at the interface is reflective of the close proximity of the IL’s melting point. The PF<sub>6</sub><sup>-</sup> anion also appears to be more conducive to structure formation than TFSA<sup>-</sup>, NO<sub>3</sub><sup>-</sup> or HCOO<sup>-</sup>, underlining the importance of molecular features related to symmetry (octahedral geometry, even charge distribution).

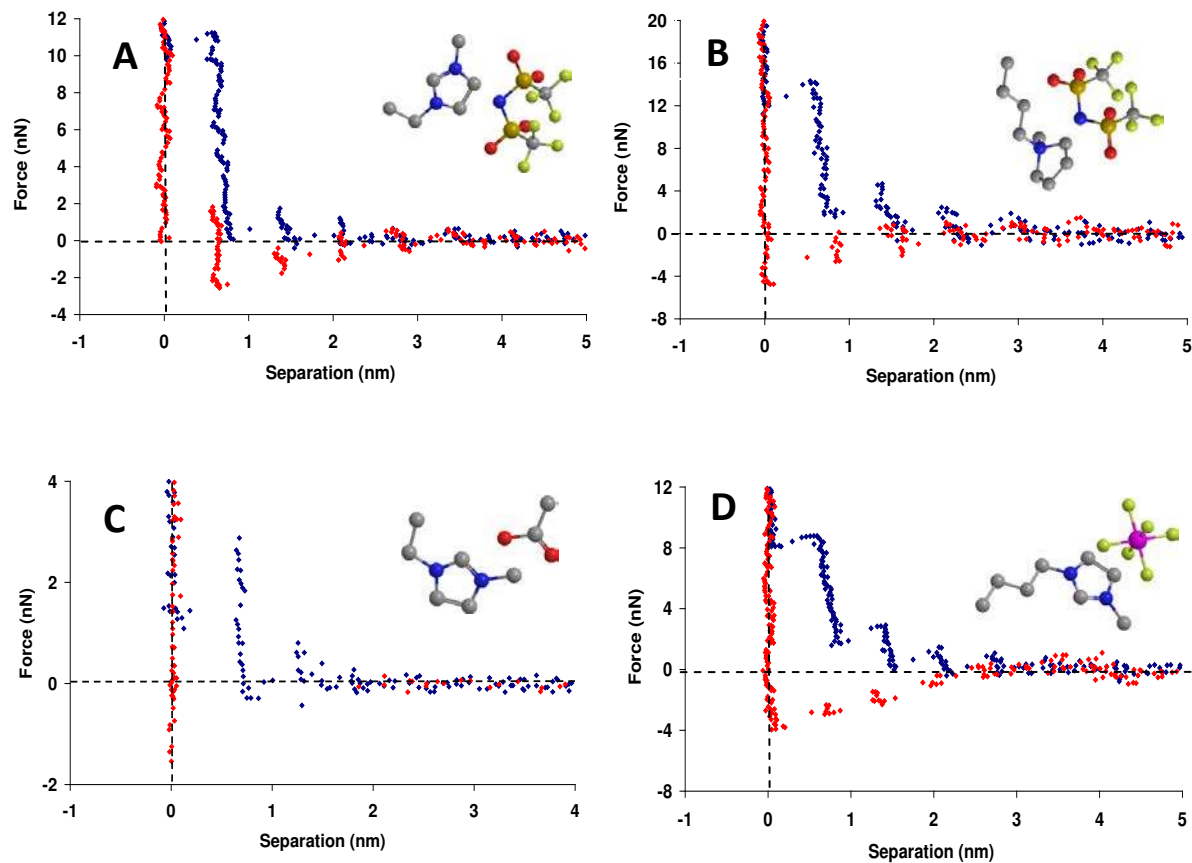


**Figure 5.** Force versus distance profile for an AFM tip approaching (blue) and retracting from (red) a mica surface in (A) [EMIm]TFSA, (B) [BMP]TFSA, (C) [EMIm]Ac and (D) [BMIm]PF<sub>6</sub> (Reproduced with permission from References [73] and [75]).

### 3.2 Silica

Silica has lower surface charge and greater roughness than mica. In water the surface charge of silica arises from hydrolysis of surface hydroxyl groups and is a function of the relative population of charged species at the surface. The surface charge density of silica is expected to be significantly higher in ILs than in water (typically one site per 20 nm<sup>2</sup> at neutral pH<sup>[145]</sup>), but still less than mica (one site per 0.48 nm<sup>2</sup><sup>[143]</sup>). The rms roughness of the silica used was determined by AFM to be 1.3 nm for a 5 x 5 μm region and 0.2 nm for a 300 x 300 nm region,

which is sufficient to broaden otherwise distinct solvation layers.<sup>[83]</sup> Roughness greater than the solvent molecular size can eliminate solvation layers completely.<sup>[123]</sup>

### ***Protic ILs on Silica***

A typical force profile for the EAN – silica system is given in Figure 6A.<sup>[78]</sup> Clear steps in the data are present but the greater roughness of the silica substrate smears the peaks considerably. A repulsive force is first measured on approach at 2.7 nm. Ensuing steps in the data are consistent with the molecular diameter of EAN, but they are slightly slanted due to compressibility imparted by surface roughness. The thinness of the innermost step (0.25 nm) suggests it consists of an electrostatically bound EA<sup>+</sup> layer, inferred but never observed for mica. As the silica is of lower surface charge density than mica, the adsorbed layer can be displaced by the AFM tip at sufficiently high force. The force profile for the retraction is quite similar to that recorded for the approach as there is negligible adhesion of the AFM tip to the surface.

The PAN – silica force curve (Figure 6B) is similar to EAN – silica in many respects. The morphology appears disordered due to surface roughness and is characterized by strong repulsive forces on approach. A distinct PA<sup>+</sup> layer is also noted which, as for EAN-silica and DMEAF-mica, can be penetrated by the AFM tip.

### ***Aprotic ILs on Silica***

The [EMIm]Ac - silica force profile is presented in Figure 6C.<sup>[78]</sup> The data resembles the surface interaction of this IL with mica (Figure 5C) and suggests an electrostatically bound interfacial layer of EMIm<sup>+</sup> cations, followed by two layers with widths consistent with the ion pair. The reduced spacing of the inner cation layer is consistent with the ethyl group being orientated approximately normal to the interface. The increased molecular volume and delocalization of

charge on  $\text{EMIm}^+$  compared to the  $\text{EA}^+$  cation means that absorption is weaker for the aprotic IL. This in turn reduces the ordering propensity of the liquid at the interface; adsorption serves to template the ensuing ion pair layer through solvophobic interactions between cations.

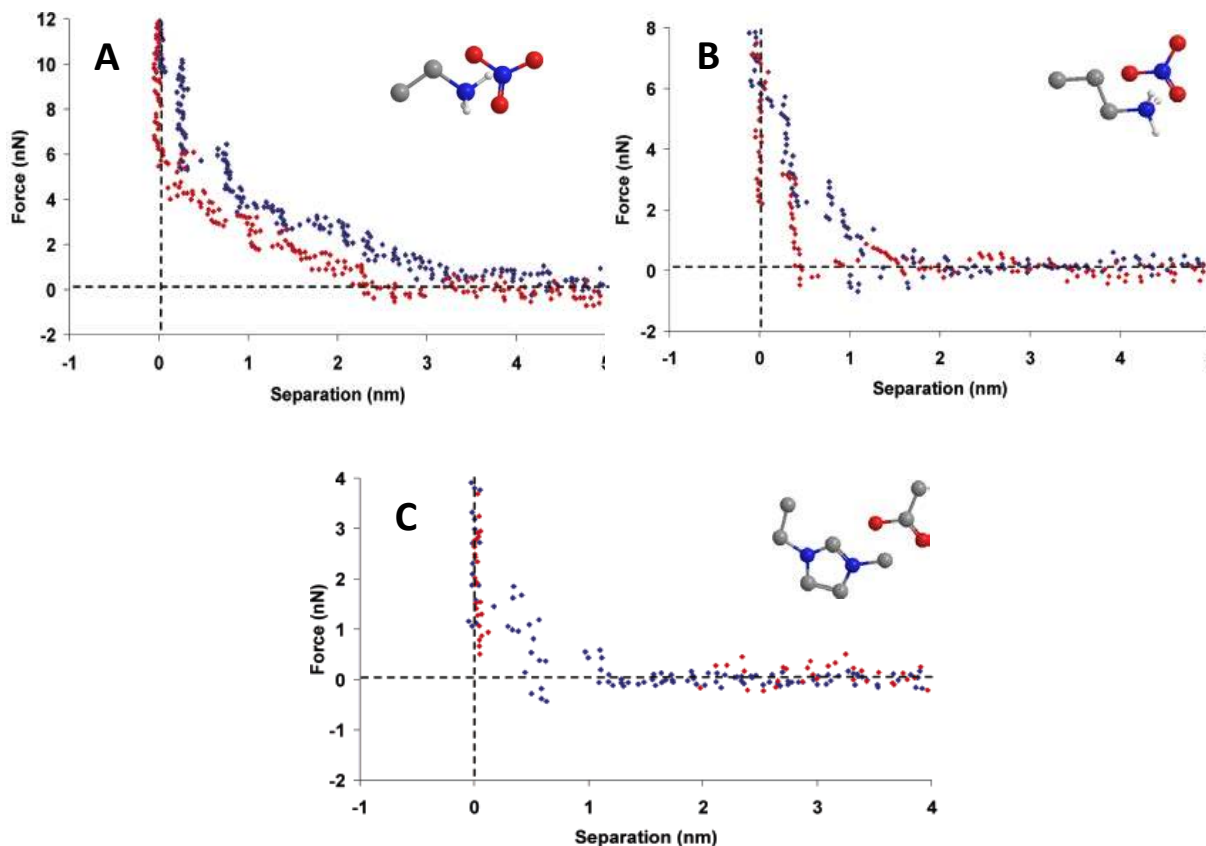


**Figure 6.** Force versus distance profile between an AFM tip approaching (blue) and retracting from (red) a silica surface in (A) EAN, (B) PAN and (C) [EMIm]Ac (Reproduced with permission from Reference [73])

Sum frequency generation (SFG) spectroscopy has also been used to investigate aprotic IL ordering at a silica interface.<sup>[88,89]</sup> Fitchett and Conboy<sup>[89]</sup> showed the imidazolium cation is absorbed first with its orientation essentially independent of the cation alkyl chain length and anion structure. The imidazolium ring was found to be slightly tilted at the silica surface (between  $16^\circ$  and  $32^\circ$ ), from the HCCH dipole orientation. However, the orientation of the cation alkyl chain was nearly normal to the solid surface. A follow-up paper by the same group

revealed two important results regarding the interfacial structure.<sup>[88]</sup> Firstly, the alkyl chain has a strong influence on the cation orientation. With decreasing alkyl chain length, the imidazolium ring tends to a more parallel surface orientation. Similar conformational order could be induced in the first cation layer when the silica charge density was increased, highlighting the importance of electrostatic interactions for IL-substrate ordering.

### 3.3 Graphite

The interfacial forces measured for both protic and aprotic ILs confined between an AFM tip and graphite are quite different to those measured for mica and silica.<sup>[78]</sup>

#### *Protic ILs on Graphite*

The EAN-graphite force profile (Figure 7A) is dominated by attractive dispersion interactions between tip and substrate on approach. The jump to contact distance can be used to estimate the Hamaker constant of the system.<sup>\*\*</sup> Three steps in the force profile are still apparent, but they are superimposed on attractive forces. Two adhesions are detected on retraction, the first of which is between tip and the surface, and the second is between the tip and the adsorbed EA<sup>+</sup> layer at a separation of 0.35 nm. Interactions between the ethyl group and graphite may produce a interfacial excess of this ion, similar to that observed for the squalene-OCMTS-graphite system.<sup>[146]</sup>

---

<sup>\*\*</sup> From the relationship  $D_j = (AR/3k)^{1/3}$  the jump distance ( $D_j$ ) can be used to estimate the Hamaker constant ( $A$ ) for this system, where  $k$  is the tip spring constant and  $R$  is the tip radius. Using measured values for  $R$  (20 nm) and  $k$  ( $0.07 \text{ N m}^{-1}$ ),  $A = 2 \times 10^{-20} \text{ J}$  is calculated. This value is higher than for other liquids, but increasing  $R$  to 40 nm gives  $A$  with the expected order of magnitude. This increase in  $R$  is reasonable given the change in tip geometry due to wear that occurs over the course of an AFM experiment.<sup>[96]</sup>

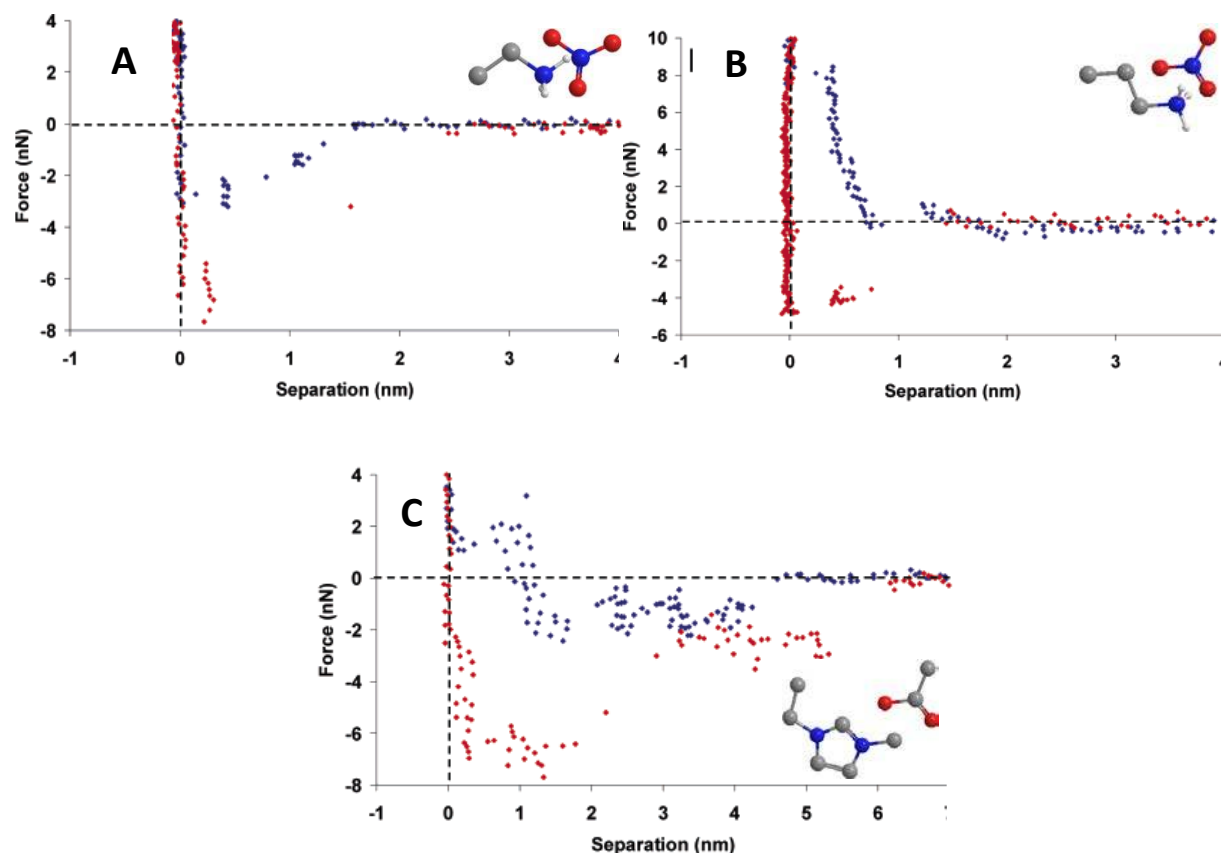


**Figure 7.** Force versus distance profile between an AFM tip approaching (blue) and retracting from (red) a graphite surface in (A) EAN, (B) PAN and (C) [EMIm]Ac at 21°C. (Reproduced with permission from Reference [73])

The force curve for the PAN-graphite system is presented in Figure 7B. A small repulsion occurs between 1.9 and 1.2 nm, followed by a jump from 1.2 to 0.75 nm on approach. Here there is a second, much steeper repulsion, with the force increasing from zero to 8 nN as the separation decreases from 0.75 to 0.35 nm. The tip then pushes through the layer into contact with the substrate. The increased size of the hydrocarbon group on PAN compared to EAN is responsible for the greater force required to rupture the interfacial layer. On graphite, cations interact with the surface via their alkyl tail group solvophobically, so PAN is more strongly bound to the surface than EAN. The final push through distance is lower than expected, due to interfacial  $PA^+$



being, orientated, on average, flat along the substrate. Similar conclusions have been drawn for n-alcohols on graphite.<sup>[129]</sup>

### ***Aprotic ILs on Graphite***

The form of the data for [EMIm]Ac – graphite (Figure 7C) is unlike any other interfacial system presented. Attractive forces are dominant on approach and retraction. The measured spacings are consistent with the predicted ion pair spacing value for [EMIm]Ac, except for the smaller final push through, resulting from surface parallel cation ring orientation. This cation alignment favors the formation of six to seven solvation layers on graphite, substantially more than on silica or mica for the same IL (where a perpendicular orientation was preferred).

## **3.4 Au(111)**

### ***Aprotic ILs on Au(111)***

Force versus separation data for [EMIm]TFSA and [BMP]TFSA confined between an AFM tip and a gold substrate are shown in Figures 8A and 8B respectively.<sup>[82]</sup> The RMS roughness of the gold surfaces was less than 0.1 nm over a 300 nm<sup>2</sup> area. The force profiles are qualitatively similar to those obtained for the same aprotic ILs on mica (Figure 5A and 5B),<sup>[80]</sup> with a series of push throughs noted at discrete separations as the AFM tip moves towards the surface.

The key difference compared to mica is that the width of the interfacial layer is smaller than predicted for the ion pair (Table 1), suggesting the innermost layer is cation rich and weakly bound, allowing the AFM tip to rupture it and move into contact with the gold substrate. For [EMIm]TFSA, a 13% reduction in layer thickness is measured, suggesting electrostatic

attractions induce the imidazolium ring of the cation to tilt towards the gold surface. Due to its short ( $C_2$ ) alkyl group, the aromatic ring on [EMIm]TFSA is expected to be orientated substantially towards the surface, much higher than [BMIm]TFSA. It is likely that the reduction in layer thickness is a result of this electrostatic alignment of the cation, and not due to an imbalance of ions.

For the [BMP]TFSA – Au(111) system (Figure 8B) the closest layer to the surface is 25 % smaller than predicted at 0.6 nm. This distance is even smaller than the innermost step measured for [EMIm]TFSA, which has a smaller molecular volume (c.f Table 1). We suggest that strong electrostatic attractions as well as the absence of an inflexible aromatic ring allow the  $BMP^+$  cation to adopt a flatter surface conformation than [EMIm]TFSA, thus resulting in the reduced layer thickness.

In every instance the rupture force of corresponding layers is greater for [BMP]TFSA than for [EMIm]TFSA. This is because the cohesive energy within layers is greater for [BMP]TFSA than [EMIm]TFSA, consistent with X-ray diffraction experiments<sup>[61]</sup> (for similar ILs) which show that the level of order increases with cation alkyl chain length. Stronger solvophobic clustering occurs as the size of the cation alkyl groups is increased, hence the greater rupture force for corresponding solvation layers. At the interface, IL-surface electrostatic interactions will also influence the force required to push through the layer nearest to the substrate. The significantly higher force required to disrupt [BMP]TFSA compared to [EMIm]TFSA is consistent with increased electrostatic interactions between the surface and the cation; the positive charge is localised on one atom in the case of  $[BMP]^+$  and delocalised across an aromatic for  $[EMIm]^+$ . These simple molecular differences result in the increased strength of the surface interaction for [BMP]TFSA compared to [EMIm]TFSA.

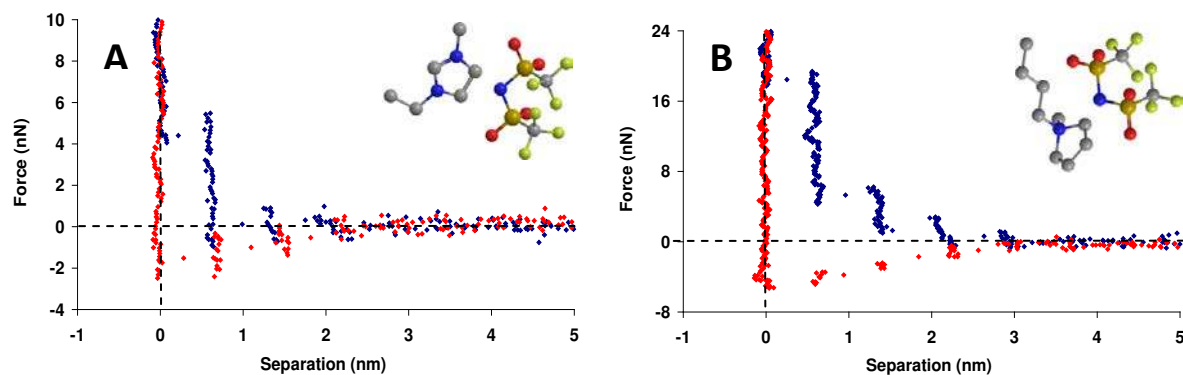


**Figure 8.** Force versus distance profile for an AFM tip approaching (blue) and retracting from (red) a gold (111) surface in (A) [EMIm]TFSA and (B) [BMP]TFSA at 21°C. (Reproduced with permission from Reference [77])

## 4 Discussion

Many IL applications depend on interfaces, in particular the solid-liquid interface. In the following section, IL research frontiers are discussed in the context of the data presented above, and avenues for further research identified.

### 4.1 Particle Stability & Heterogeneous Catalysis

Nanoparticle catalysts are attractive for chemical synthesis on account of their high surface area to volume ratio. The colloid stability in aqueous systems is determined by the balance between attractive van der Waals and repulsive electrostatic interactions, which are mediated by the electrolyte concentration. But in ILs, electrostatic repulsions between charged particles are screened by the high ionic strength e.g. EAN is 11 M salt, leading to a Debye length of only  $\sim 1$  Å. Thus particle suspensions should not be stable in ILs, yet several studies report particle stability in ILs in the absence of stabilizers.<sup>[52,55,147-152]</sup> It appears that IL structure induced in the

vicinity of the solid nanoparticle produces solvation forces that are sufficient to prevent aggregation. This is exemplified by the results obtained by Dupont *et al.*<sup>[52]</sup> which show that metallic nanoparticles can be synthesized and stabilized in ILs, consistent with the AFM results presented in Section 3. X-ray Diffraction and Small Angle X-ray Scattering showed that the IL formed a ‘protective layer’ surrounding the transition-metal nanoparticle surface. Layers extended 2.8-4.0 nm from the surface depending on the anion. These distances are much too large to be due to a single layer of ions or ion pairs, but are completely consistent with the range of solvation forces measured using AFM. A follow-up study by Schrekker *et al.*<sup>[55]</sup> used surface-enhanced Raman spectroscopy to elucidate the coordination structure of the adsorbed cation on Au(0). The imidazolium ring was found to orient parallel to the surface, and the alkyl chain projected away from the nanoparticle, reminiscent of surfactant steric stabilization.

IL heterogeneous catalytic schemes, such as Supported Ionic Liquid Catalysis (SILC),<sup>[153,154]</sup> will similarly be affected by interfacial structure. SILC uses a surface modified with a monolayer of covalently attached IL fragments. Subsequent addition of IL will result in the formation of solvation layers. As the active catalyst is dissolved in the IL phase and the reactant in another immiscible liquid, the presence of interfacial layers at the solid-liquid and air-liquid interfaces are expected to influence the catalytic properties of the system.

## 4.2 Dye-Sensitized Solar Cells

ILs have been extensively used as electrolytes for dye-sensitized solar cells.<sup>[47]</sup> In addition to challenges associated with transport properties due to high IL viscosity, little is known about the structure of the photoactive titania – dye – IL interface.<sup>[47]</sup> As the dye is located at the solid-electrolyte interface, control of IL structure within the solvation zone (and the resultant transport

properties arising from it) is crucial to optimizing performance. Recent experiments by our group<sup>[155]</sup> have shown that, like other solid substrates, solvation layers form at the titania – dye – IL interface. This is likely to slow transfer of the redox couple to the interface, as there are distinct barriers (which become increasingly stronger closer to the interface) impeding motion. However, Yamanaka *et. al.*<sup>[156,157]</sup> have used an ionic liquid crystal to counter undesirable IL-viscosity effects. Solvophobic self-assembly of IL cations results in a bilayer architecture conducive to redox-couple reactions and leads to high conversion efficiencies and short circuit densities.

### **4.3 Electrochemistry**

The results presented in section 3 revealed that the number of solvation layers present and the strength of surface – cation interactions are functions of IL species. This interfacial structure could, on the one hand, prevent imaging of metal electrodes with atomic resolution by probe microscopy, but also influence electrochemical processes by controlling the rate of diffusion of species to and from the interface; strong surface-cation interactions could also prevent adsorption of redox species. The interfacial structure of several useful IL solvents has been reviewed above, and general rules developed for predicting the level of interfacial structure. It should now be possible to systematically investigate the effect of IL structure on electrochemical performance. Future work should investigate how solvation layers are affected by (1) dissolved electrolyte (2) an applied potential (3) temperature.

### **4.4 Lubrication**

Due to strong ion adsorption at solid surfaces, lubrication and other tribological applications of ILs shows great promise.<sup>[48,158]</sup> Robust physicochemical properties, in particular negligible vapour pressure, could lead to important niche applications, such as in vacuum environments where ILs could be used without significant product loss. In the context of this Perspective Review, the tendency for ILs to adsorb and spontaneously arrange into solvation layers results in a coating of ions at the solid interface. Whilst the heat generated from friction could disrupt layering, a densely-packed monolayer of adsorbed cations at the surface would prevent contact between the surfaces of moving parts. Previous studies on a steel surface<sup>[159,160]</sup> have shown the friction coefficient decreases with increasing cation chain length; solvophobic interactions produce discrete charged and apolar layers at the surface, similar to the Bowden-Tabor<sup>[161]</sup> mechanism for solid lubrication. However, Minami recently cautioned that the thermo-oxidative stability of ILs decreases with longer alkyl chain lengths, which can lead to tribochemical reactions under extreme temperature and pressures.<sup>[158]</sup> Whilst protic ILs are susceptible to thermal degradation<sup>[13]</sup> (and are therefore probably unsuitable for lubrication applications), aprotic ILs with localized charge centers and relatively long alkyl chains should be relatively unreactive and have been shown to interact strongly with solid surfaces.

#### **4.5 Analytical Applications**

ILs are a new and relatively underused class of solvents for analytical chemistry (sample preparation, chromatography and detection).<sup>[162]</sup> Because ILs possess a so-called ‘dual’ chemical nature<sup>[163]</sup> (i.e. discrete polar and apolar regions in the bulk), upon dissolution, analytes are spontaneously separated into domains of like molecular groups.<sup>[164-166]</sup> Thus, a strong foundation

for IL use in quantitative and qualitative separations processes<sup>[33,162,163,167]</sup> is present, the difficulty lies in harnessing this for quantitative applications.

One area where ILs have been incorporated into existing technologies to great effect is in gas<sup>[163]</sup> and liquid<sup>[168]</sup> chromatography. The IL cation is expected to strongly interact with the surface hydroxyl groups of the silica column and, at sufficient concentrations, template solvation layers. This leads to a competition between the IL and analyte molecular groups for the silica surface as suggested by He *et. al.*<sup>[169]</sup> Moreover, there should also be a parameter related to how well each analyte is incorporated into solvation layers. These results suggest ILs could be useful additives to the eluent to improve separation.

ILs that are immiscible with water or organic solvents find use in two-phase liquid-liquid extractions. Knowledge of the likely liquid-IL interface structure means that suggestions for designing ILs can be made. The alkyl group of interfacial cations will orientate towards hydrophobic solvents to lower the surface energy of the interface, similar to results present above for solid graphite. This explains results for metal-ion extraction from aqueous solution.<sup>[170]</sup> By incorporating chelating functional groups on the ends of the cation alkyl chain, the cation is able to reach into solution and bind with the target species. As the monolayer is a dynamic system, cations that have successfully bound a metal ion are continuously being replaced with bulk cations, facilitating high yields / distribution coefficients that favor the IL. The challenge now is to optimize the mass transport properties of the system by limiting the extent to which IL solvation layers form at the liquid-liquid interface. As demonstrated from the AFM results, this could be achieved in a number of ways, such as reducing the length of alky chain, raising the temperature, etc.

## 4.6 Liquid and Solid IL Phases Coexisting?

Three recent AFM tapping-mode studies have suggested that IL liquid and solid phases coexist on mica,<sup>[171,172]</sup> silica,<sup>[108,172]</sup> and graphite<sup>[172]</sup> surfaces at room temperature. Liu *et al.*<sup>[171]</sup> and Bovio *et al.*<sup>[108,172]</sup> diluted ILs in methanol (to ~ 0.5wt%) and then probed the subsequent solid-liquid interface after methanol evaporation. Topographical images revealed solid islands 1-100  $\mu\text{m}^2$  in areas and upwards of 50 nm thick. Apart from computer simulations by the same authors,<sup>[108-110]</sup> to our knowledge no evidence of solid phase formation has been observed in any pure IL-solid interface system. These studies are reminiscent of early AFM investigations of surfactant adsorbed layers, in which the equilibrium adsorbed layer structure was rather different from that observed by evaporative deposition. Nevertheless this effect clearly warrants further investigation.

## 5. Summary & Outlook

The AFM results reviewed herein allow us to clearly describe interfacial IL structure, and suggest design rules for tailoring IL behaviour for a given interfacial application. IL near-surface structure is unlike conventional liquids in many ways, and responsive to specific molecular, liquid and surface effects.

The key difference between IL interfacial structure and classical molecular liquid solvation layers is that many ILs possess bulk order; whereas conventional solvents may have preferred organization of adjacent molecules, in ILs this order can be propagated over much greater distances, often in the form of a disordered sponge ( $L_3$  phase) structure<sup>[62,67]</sup> where the ions form a network of polar and non-polar domains due to electrostatic and solvophobic clustering of like



molecular groups. As the intermolecular forces that generate bulk nanostructure are still present at the interface, the tendency to self-assemble is not diminished. It is not a coincidence that ILs with strong bulk organization also have strong near surface structure, and *vice versa*; at a solid interface the ILs polar and non-polar domains persist, but the presence of the surface induces a more ordered lamellar like structure.

The nature of the IL-surface interaction also influences interfacial organization. Cations are electrostatically adsorbed to negatively charged surfaces (mica, silica, Au(111)). The interaction strength is determined by the surface charge, the cation charge localization/delocalization, and the degree of substitution around the charge centre. As the surface and charge group distance is greater for substituted cations, and Coulombic forces decrease with the square of distance, substituted cations are much less strongly bound to negatively charged surfaces. For graphite, solvation forces are superimposed on an attractive van der Waals force. However, it is clear that solvophobic interactions between cation alkyl chains and the substrate are important, and the chain appears to lie flat on the surface. The strength with which the cation is bound to the surface increases with the length of the cation alkyl chain.

Surface roughness affects the level of interfacial order for both molecular solvents and ILs. For ILs, substrate smoothness is vital for strong interfacial organization, as the intermolecular forces that promote clustering of apolar regions are short range. Molecular flexibility within ionic groups also determines interfacial order, and in some instances is more important than the level of bulk order. For example, the intensity of the peak in the SANS spectra of PAN is greater than that of EAN, suggesting bulk order is more pronounced for PAN. However, at the interface, the additional flexibility imparted by the longer alkyl chain results in fewer and more compressible layers for PAN than EAN.

In summary, at an atomically smooth, charged surface IL interfacial organization is as follows. The innermost layer is cation rich,<sup>[104]</sup> held in place by strong Coulombic forces (sometimes so strong that it cannot be displaced by a sharp AFM tip). The next layer is also composed of cations, with alkyl groups oriented towards the surface to interact solvophobicly with surface bound cations. This is followed by alternating ionic and apolar layers. As the interfacial cation layer is macroscopically flat due to the surface, the sponge structure of the bulk transforms to a lamellar phase at the interface. This lamellar architecture eventually decays into the bulk sponge structure, with the rate of decay reflective of both the level of bulk order and molecular flexibility. Corresponding surface ordering has been reported for aqueous surfactant sponge phases.<sup>[173]</sup>

The ability to predictably tune the level of interfacial structure via structural variation in the IL cation and anion means ILs can be tailored for optimal performance in a given application.

Where mobility of component ions and transfer of species to and from the interface is required (e.g. dye-sensitised solar cells,<sup>[47]</sup> heterogeneous catalysis<sup>[44]</sup> etc.) multiple sterically-hindered alkyl groups could be incorporated to minimise substrate – IL interactions and maximise compressibility of the solvation layers. Conversely, in situations where IL adsorption to the interface is desirable (eg. lubrication,<sup>[48]</sup> electrode surface restructuring<sup>[174]</sup>) symmetric ions with localized charge centers are preferable, particularly for the cation.

## **Acknowledgments**

This work was supported by an Australian Research Council (ARC) Discovery Project and the Access to Major Research Facilities program. RH thanks the University of Newcastle Faculty of

Science and Information Technology for provision of an Honours research scholarship. RA wishes to acknowledge the University of Newcastle for a Research Fellowship.

## References

- (1) Reichardt, C. *Solvents and solvent effects in organic chemistry*, 3rd ed.; VCH: Weinheim, 2003.
- (2) Rogers, R. D. *Nature* **2007**, *447*, 917.
- (3) Belieres, J.-P.; Angell, C. A. *J. Phys. Chem. B* **2007**, *111*, 4926.
- (4) Wilkes, J. S. *Green Chem.* **2002**, *4*, 73.
- (5) Hussey, C. L. The electrochemistry of room-temperature haloaluminate molten salts. In *Chemistry of Nonaqueous Solutions*; Mamantov, G., Popov, A. I., Eds.; VCH Publisher Inc.: New York, 1994; pp 227.
- (6) Seddon, K. R. *Journal of Chemical Technology & Biotechnology* **1997**, *68*, 351.
- (7) Freemantle, M. *Chem. Eng. News* **1998**, *76*, 32.
- (8) Welton, T. *Chem. Rev.* **1999**, *99*, 2071.
- (9) Rogers, R. D.; Seddon, K. R. *Science* **2003**, *302*, 792.
- (10) Anastas, P. T.; Warner, J. C. *Green chemistry: theory and practice*; Oxford University Press: New York, 2000.
- (11) Earle, M. J.; Seddon, K. R. *Pure & Applied Chemistry* **2000**, *72*, 1391.
- (12) Rogers, R. D.; Seddon, K. R.; Volkov, S. *Green Industrial Applications of Ionic Liquids*; Kluwer Academic: Dordrecht, Netherlands, 2003.
- (13) Greaves, T. L.; Weerawardena, A.; Fong, C.; Krodkiewska, I.; Drummond, C. J. *J. Phys. Chem. B* **2006**, *110*, 22479.
- (14) Wishart, J. F.; Castner, E. W. *J. Phys. Chem. B* **2007**, *111*, 4639.
- (15) Greaves, T. L.; Drummond, C. J. *Chem. Rev.* **2008**, *1088*, 206.
- (16) Endres, F.; Zein El Abedin, S. *Phys. Chem. Chem. Phys.* **2006**, *8*, 2101.
- (17) Earle, M. J.; Esperanca, J. M. S. S.; Gilea, M. A.; Canongia Lopes, J. N.; Rebelo, L. P. N.; Magee, J. W.; Seddon, K. R.; Widegren, J. A. *Nature* **2006**, *439*, 831.
- (18) Yoshizawa, M.; Xu, W.; Angell, C. A. *J. Am. Chem. Soc.* **2003**, *125*, 15411.
- (19) Forsyth, S. A. P., J. M.; Macfarlane, D. R. *Aust. J. Chem.* **2004**, *57*, 113.
- (20) Cull, S. G.; Holbrey, J. D.; Vargas-Mora, V.; Seddon, K. R.; Lye, G. J. *Biotechnology and Bioengineering* **2000**, *69*, 227.
- (21) Marsh, K. N.; Deev, A.; Wu, A. C.-T.; Tran, E.; Klamt, A. *Korean J. Chem. Eng.* **2002**, *19*, 357.
- (22) Walden, P. *Bull. Acad. Imper. Sci.* **1914**, 1800.
- (23) Rogers, R. D.; Bica, K.; Gurau, G.; Smiglak, M.; Rodriguez, H.; Shamshina, J. "Ionic Liquids at the Intersections"; Congress on Ionic Liquids III, 2009, Carins.
- (24) Hamaguchi, H.; Ozawa, R. *Adv. Chem. Phys.* **2005**, *131*, 85.
- (25) Hamaguchi, H. "Nanoscope structure of Ionic Liquids"; Congress on Ionic Liquids III, 2009, Carins.
- (26) Xu, W.; Cooper, E. I.; Angell, C. A. *J. Phys. Chem. B* **2003**, *107*, 6170.
- (27) Yamamuroa, O.; Minamimotoua, Y.; Inamuraa, Y.; Hayashib, S.; Hamaguchi, H. *Chem. Phys. Lett.* **2006**, *423*, 371.
- (28) Zein El Abedin, S.; Endres, F. *Acc. Chem. Res.* **2007**, *40*, 1106.
- (29) Marcus, Y. *Solvent Mixtures*; Marcel Decker: New York, 2002.

- (30) Canongia Lopez, J. N.; Rebelo, L. P. N.; Costa Gomes, M. F.; Padua, A. A. H. "Ionic Liquid Liquids, Solids and Gases: Phase Diagrams from a molecular Perspective"; Congress on Ionic Liquids III, 2009, Carins.
- (31) Angell, C. A.; Byrne, N.; Belieres, J.-P. *Acc. Chem. Res.* **2007**, *40*, 1228.
- (32) Baudequina, C.; Baudouxa, J.; Levillainb, J.; Caharda, D.; Gaumont, A. E.; Plaquevent, J. C. *Tetrahedron: Asymmetry* **2003**, *14*, 3081.
- (33) Ding, J.; Armstrong, D. W. *Chirality* **2005**, *17*, 281.
- (34) Evans, D. F.; Chen, S. H.; Schriver, G. W.; Arnett, E. M. *J. Am. Chem. Soc.* **1981**, *103*, 481.
- (35) Evans, D. F.; Yamauchi, A.; Roman, R.; Casassa, E. Z. *J. Colloid Interface Sci.* **1982**, *88*, 89.
- (36) Evans, D. F.; Yamauchi, A.; Wei, G. J.; Bloomfield, V. A. *J. Phys. Chem.* **1983**, *87*, 3735.
- (37) Fumino, K.; Wulf, A.; Ludwig, R. *Angew. Chem. Int. Ed.* **2009**, *48*, 3184.
- (38) MacFarlane, D. R.; Seddon, K. R. *Aust. J. Chem.* **2007**, *60*, 3.
- (39) Davis, J. H. J.; Gordon, C. M.; Hilgers, C.; Wasserscheid, P. Chapter 2: Synthesis and Purification of Ionic Liquids. In *Ionic liquids in synthesis*; Wasserscheid, P., Welton, T., Eds.; Wiley-VCH Verlags GmbH: Weinheim, 2007.
- (40) Beyersdorff, T.; Schubert, T. J. S.; Welz-Biermann, U.; Pitner, W.; Abbott, A. P.; McKenzie, K. J.; Ryder, K. S. Chapter 2: Synthesis of Ionic Liquids. In *Electrodeposition from Ionic Liquids*; Endres, F., MacFarlane, D. R., Abbott, A. P., Eds.; Wiley-VCH, 2008.
- (41) Cooper, E. I.; O'Sullivan, E. J. Proc. 8th. Intern. Symp. Molten Salts, Electrochemical Soc., 1992, Pennington NJ; Vol 92-16, p 386.
- (42) Wilkes, J. S.; Zaworotko, M. J. *J. Chem. Soc., Chem. Commun.* **1992**, 965.
- (43) Chiappe, C. Chapter 5: Organic Synthesis. In *Ionic liquids in synthesis*; 2nd ed.; Wasserscheid, P., Welton, T., Eds.; Wiley-VCH Verlags GmbH: Weinheim, 2007.
- (44) Parvulescu, V. I.; Hardacre, C. *Chem. Rev.* **2007**, *107*, 2615.
- (45) Endres, F. *ChemPhysChem* **2002**, *3*, 144.
- (46) Zein El Abedin, S.; Moustafa, E.; Hempelmann, R.; Natter, H.; Endres, F. *ChemPhysChem.* **2006**, *7*, 1535.
- (47) Gorlov, M.; Kloo, L. *Dalton Trans.* **2008**, 2655
- (48) Ye, C.; Lui, W.; Chen, Y.; Yu, L. *Chem. Commun.* **2001**, 2244
- (49) Carmichael, A. J.; Haddleton, D. M. Chapter 7: Polymer Synthesis in Ionic Liquids. In *Ionic liquids in synthesis*; Wasserscheid, P., Welton, T., Eds.; Wiley-VCH, 2007.
- (50) Booker, K.; Bower, M. C.; Lennard, C. J.; Holdsworth, C. I.; McCluskey, A. *Chem. Commun.* **2006**, *1*, 1730.
- (51) Kim, J. Y.; Kim, J. T.; Song, E. A.; Min, Y. K.; Hamaguchi, H. *Macromolecules* **2008**, *41*, 2886.
- (52) Dupont, J.; Fonseca, G. S.; Umpierre, A. P.; Fichtner, P. F. P.; Teixeira, S. R. *J. Am. Chem. Soc.* **2002**, *124*, 4228.
- (53) Machado, G.; Scholten, J. D.; de Vargas, T.; Teixeira, S. R.; Ronchi, L. H.; Dupont, J. *International Journal of Nanotechnology* **2005**, *4*, 541.
- (54) Antonietti, M.; Kuang, D.; Smarsly, B.; Zhou, Y. *Angew. Chem. Int. Ed.* **2004**, *43*, 4988.
- (55) Schrekker, H. S.; Geleskya, M. A.; Strackea, M. P.; Schrekker, C. M. L.; Machadoa, G.; Teixeira, S. R.; Rubim, J. C.; Dupont, J. *J. Colloid Interface Sci.* **2007**, *316*, 189.
- (56) Barisci, J. N.; Wallace, G. G.; MacFarlane, D. R.; Baughman, R. H. *Electrochem. Comm.* **2004**, *6*, 22.
- (57) Shim, Y.; Kim, H. J. *ACS Nano* **2009**, *3*, 1693.
- (58) Eastoe, J.; Gold, S.; Rogers, S. E.; Paul, A.; Welton, T.; Heenan, R. K.; Grillo, I. *J. Am. Chem. Soc.* **2005**, *127*, 7302.
- (59) Atkin, R.; Warr, G. G. *J. Phys. Chem. B* **2007**, *111*, 9309.

- (60) Qiu, Z.; Texter, J. *Curr. Opin. Colloid Interface Sci.* **2008**, *13*, 252.
- (61) Triolo, A.; Russina, O.; Bleif, H. J.; Di Cola, E. *J. Phys. Chem. B* **2007**, *111*, 4641.
- (62) Atkin, R.; Warr, G. G. *J. Phys. Chem. B* **2008**, *112*, 4164
- (63) Umebayashi, Y.; Chung, W.; Mitsugi, T.; Fukuda, S.; Takeuchi, M.; Fujii, K.; Takamuku, T.; Kanzaki, R.; Ishiguro, S. *J. Comput. Chem. Jpn.* **2008**, *7*, 125.
- (64) Xiao, D.; Rajian, J. R.; Hines, L. G.; Li, S.; Bartsch, R. A.; Quitevis, E. L. *The Journal of Physical Chemistry B* **2008**, *112*, 13316.
- (65) Triolo, A.; Russina, O.; Fazio, B.; Triolo, R.; Di Cola, E. *Chemical Physics Letters* **2008**, *457*, 362.
- (66) Iwata, K.; Okajima, H.; Saha, S.; Hamaguchi, H. *Acc. Chem. Res.* **2007**, *40*, 1174.
- (67) Atkin, R.; Wakeham, D.; Hayes, R.; Imberti, S.; Warr, G. G. "Bulk and Interfacial Nanostructure in Ionic Liquids"; Congress on Ionic Liquids III, 2009, Cairns.
- (68) Xiao, D.; Rajian, J. R.; Hines, L. G.; Li, S.; Bartsch, R. A.; Quitevis, E. L. *J. Phys. Chem. B* **2007**, *112*, 13316.
- (69) Wang, Y.; Voth, G. A. *Journal of the American Chemical Society* **2005**, *127*, 12192.
- (70) Canongia Lopes, J. N.; Costa Gomes, M. F.; Padua, A. A. H. *J. Phys. Chem. B* **2006**, *110*, 16818.
- (71) Bhargava, B. L.; Balasubramanian, S.; Klein, M. L. *Chem. Commun.* **2008**, 3339.
- (72) Urahata, S. M.; Ribeiro, M. C. C. *J. Chem. Phys.* **2004**, *120*, 1855.
- (73) Ray, A. *Nature* **1971**, *231*, 313.
- (74) Davis, J. H. *Chem. Lett.* **2004**, *33*, 1072.
- (75) Tokuda, H.; Hayamizu, K.; Ishii, K.; Abu Bin Hasan Susan, M.; Watanabe, M. *J. Phys. Chem. B* **2005**, *109*, 6103.
- (76) Greaves, T. L.; Weerawardena, A.; Fong, C.; Krodkiewska, I.; Drummond, C. J. *The Journal of Physical Chemistry B* **2006**, *110*, 22479.
- (77) Corey, E. J.; Cheng, X. M. *The Logic of Chemical Synthesis*; Wiley: New York 1995
- (78) Atkin, R.; Warr, G. G. *J. Phys. Chem. C* **2007**, *111*, 5162.
- (79) Wakeham, D.; Hayes, R.; Warr, G. G.; Atkin, R. *J. Phys. Chem. B* **2009**, *113*, 5961.
- (80) Hayes, R.; El Abedin, S. Z.; Atkin, R. *J. Phys. Chem. B* **2009**, *113*, 7049.
- (81) Atkin, R.; Warr, G. G. Bulk and Interfacial Nanostructure in Protic Room Temperature Ionic Liquids. In *Ionic Liquids V: From Knowledge to Application*; Plechkova, N., Seddon, K. R., Rogers, R. D., Eds.; American Chemical Society, 2009.
- (82) Atkin, R.; El Abedin, S. Z.; Hayes, R.; Gasparotto, L. H. S.; Borisenko, N.; Endres, F. *J. Phys. Chem. C* **2009**, *113*, 13266.
- (83) Isrelachvili, J. N. *Intermolecular and Surface Forces*; Academic Press: London, 1992.
- (84) Hiemenz, P. C.; Rajagopalan, R. *Principles of colloid and surface chemistry*, 3rd ed.; CRC, 1997.
- (85) Atkin, R.; Craig, V. S. J.; Wanless, E. J.; Biggs, S. *Advances in Colloid and Interface Science* **2003**, *103*, 219.
- (86) Atkin, R.; Warr, G. G. *J. Am. Chem. Soc.* **2005**, *127*, 11940.
- (87) Atkin, R.; De Fina, L.-M.; Kiederling, U.; Warr, G. G. *J. Phys. Chem. B* **2009**, *113*, 12201.
- (88) Rollins, J. B.; Fitchett, B. D.; Conboy, J. C. *J. Phys. Chem. B* **2007**, *111*, 4990.
- (89) Fitchett, B. D.; Conboy, J. C. *J. Phys. Chem. B* **2004**, *108*, 20255.
- (90) Romero, C. R.; Baldelli, S. *J. Phys. Chem. B* **2006**, *110*, 6213.
- (91) Romero, C. R.; Moore, H. J.; Lee, T. R.; Baldelli, S. *J. Phys. Chem. C* **2007**, *111*, 240.
- (92) Baldelli, S. *J. Phys. Chem. B* **2005**, *109*, 13049.
- (93) Aliaga, C.; Baldelli, S. *J. Phys. Chem. B* **2006**, *110*, 18481.
- (94) Rivera-Rubero, S.; Baldelli, S. *J. Phys. Chem. B* **2004**, *108*, 15133.

- (95) Baldelli, S. *Acc. Chem. Res.* **2008**, *41*, 421.
- (96) Aliaga, C.; Baldelli, S. *J. Phys. Chem. C* **2008**, *112*, 3064.
- (97) Rivera-Rubero, S.; Baldelli, S. *J. Phys. Chem. B* **2006**, *110*, 15499.
- (98) Iimori, T.; Iwahashi, T.; Kanai, K.; Seki, K.; Sung, J.; Kim, D.; Hamaguchi, H.-o.; Ouchi, Y. *The Journal of Physical Chemistry B* **2007**, *111*, 4860.
- (99) Rivera-Rubero, S.; Baldelli, S. *J. Phys. Chem. B* **2006**, *110*, 4756.
- (100) Jeon, Y.; Sung, J.; Bu, W.; Vakin, D.; Ouchi, Y.; Kim, D. *J. Phys. Chem. C* **2008**, *112*, 19649.
- (101) Aliaga, C.; Baker, G. A.; Baldelli, S. *J. Phys. Chem. B* **2008**, *112*, 1676.
- (102) Sloutskin, E.; Ocko, B. M.; Tamam, L.; Kuzmenko, I.; Gog, T.; Deutsch, M. *J. Am. Chem. Soc.* **2005**, *127*, 7796.
- (103) Carmichael, A. J.; Hardacre, C.; Holbrey, J. D.; Nieuwenhuyzen, M.; Seddon, K. R. *Molecular Physics* **2001**, *99*, 795.
- (104) Mezger, M.; Schroder, H.; Reichert, H.; Schramm, S.; Okasinski, J. S.; Schoder, S.; Honkimaki, V.; Deutsch, M.; Ocko, B. M.; Ralston, J.; Rohwerder, M.; Stratmann, M.; Dosch, H. *Science* **2008**, *322*, 424.
- (105) Mezger, M.; Schramm, S.; Schroder, H.; Reichart, H.; Deutsch, M.; De Souza, E. J.; Okasinski, J. S.; Ocko, B. M.; Honkimaki, V.; Dosch, H. *J. Chem. Phys.* **2009**, *131*, 094701.
- (106) Bowers, J.; Vergara-Gutierrez, M. C.; Webster, J. R. P. *Langmuir* **2003**, *20*, 309.
- (107) Pinilla, C.; Del Popolo, M. G.; Lynden-Bell, R. M.; Kohanoff, J. *J. Phys. Chem. B* **2005**, *109*, 17922.
- (108) Bovio, S.; Podesta, A.; Milani, P.; Ballone, P.; Popolo, M. G. *J. Phys.: Condens. Matter* **2009**, *21*, 424118.
- (109) Maolin, S.; Guozhong, W.; Haiping, F.; Guanglai, Z.; Yusheng, L. *J. Phys. Chem. C* **2008**, *112*, 18584.
- (110) Maolin, S.; Guozhong, W.; Yusheng, L.; Zhongfeng, T.; Haiping, F. *J. Phys. Chem. C* **2009**, *113*, 4618.
- (111) Lynden-Bell, R. M.; Del Popolo, M. G.; Youngs, T. G. A.; Kohanoff, J.; Hanke, C. G.; Harper, J. B.; Pinilla, C. *Accounts of Chemical Research* **2007**, *40*, 1138.
- (112) Lynden-Bell, R. M.; Del Popolo, M. *Phys. Chem. Chem. Phys.* **2006**, *8*, 949.
- (113) Tamford, C. A. *The Hydrophobic Effect: Formation of Micelles and Biological Membranes*, 2nd ed.; Wiley: New York, 1980.
- (114) Butt, H.-J.; Cappella, B.; Kappl, M. *Surface Science Reports* **2005**, *59(1-6)*, 152.
- (115) Cappella, B.; Dietler, G. *Surface Science Reports* **1999**, *34*, 1.
- (116) Boinovich, L. B.; Emelyanenko, A. M. *Progr. Colloid Polym. Sci.* **1999**, *112*, 64.
- (117) Abraham, F. F. *J. Chem. Phys.* **1978**, *68*, 3713.
- (118) Snook, I. K.; Henderson, D. *J. Chem. Phys.* **1978**, *68*, 2134.
- (119) Lane, J. E.; Spurling, T. H. *Chem. Phys. Lett.* **1979**, *67*, 107.
- (120) van Megen, W.; Snook, I. K. *J. Chem. Soc. Faraday Trans. II* **1979**, *7*, 1095.
- (121) van Megen, W.; Snook, I. K. *J. Chem. Phys.* **1981**, *74*, 1409.
- (122) Chan, D. Y. C.; Mitchell, D. J.; Ninham, B. W.; Pailthorpe, B. A. *Mol. Phys.* **1978**, *35*, 1669.
- (123) Horn, R. G.; Israelachvili, J. N. *J. Chem. Phys.* **1981**, *75*, 1400.
- (124) Christenson, H. K. *J. Chem. Phys.* **1983**, *78*, 6906.
- (125) Christenson, H. K.; Horn, R. G. *J. Colloid Interface Sci.* **1984**, *103*, 50.
- (126) Lim, L. T.; Wee, A. T.; O'Shea, S. J. *J. Chem. Phys.* **2009**, *130*, 134703.
- (127) Han, W.; Lindsay, S. M. *Appl. Phys. Lett.* **1998**, *72*, 1656.
- (128) Kanda, Y.; Iwasaki, S.; Higashitani, K. *J. Colloid Interface Sci.* **1999**, *216*, 394.
- (129) Franz, V.; Butt, H.-J. *J. Phys. Chem. B* **2002**, *106*, 1703.
- (130) Lim, R.; O'Shea, S. J. *Phys. Rev. Lett.* **2002**, *88*, 246101.

- (131) Thordarson, P.; Atkin, R.; Kalle, W. H. J.; Warr, G. G.; Braet, F. *Aust. J. Chem.* **2006**, *59*, 359.
- (132) Warr, G. G. *Curr. Opin. Colloid Interface Sci.* **2000**, *5*, 88.
- (133) Binnig, G.; Quate, C. F.; Gerber, C. *Physical Review Letters* **1986**, *56*, 930.
- (134) Gan, Y. *Surface Science Reports* **2009**, *64*, 99.
- (135) Notley, S. M.; Biggs, S.; Craig, V. S. J. *Rev. Sci. Instrum.* **2003**, *74*, 4026.
- (136) O'Shea, S. J.; Welland, M. E. *Langmuir* **1998**, *14*, 4186.
- (137) Senden, T. J. *Curr. Opin. Colloid Interface Sci.* **2001**, *6*, 95.
- (138) Drake, B.; Prater, C. B.; Weisenhorn, A. L.; Gould, S. A. C.; Albrecht, T. R.; Quate, C. F.; Cannell, D. S.; Hansma, H. G.; Hansma, P. K. *Science* **1989**, *243*, 1586.
- (139) Gelb, L. D.; Lynden-Bell, R. M. *Chem. Phys. Lett.* **1993**, *211*, 328.
- (140) Gelb, L. D.; Lynden-Bell, R. M. *Phys. Rev. B* **1994**, *49*, 2058.
- (141) Patrick, D. L.; Lynden-Bell, R. M. *Surf. Sci.* **1997**, *380*, 224.
- (142) Horn, R. G.; Evans, D. F.; Ninham, B. W. *J. Phys. Chem.* **1988**, *92*, 3531.
- (143) Patrick, H. N.; Warr, G. G.; Manne, S.; Aksay, I. A. *Langmuir* **1997**, *13*, 4349.
- (144) Choudhury, A. R.; Winterton, N.; Steiner, A.; Cooper, A. I.; Johnson, K. A. *J. Am. Chem. Soc.* **2005**, *127*, 16792.
- (145) Iler, R. K. *The Chemistry of Silica*; Wiley-Interscience Publishers: New York, 1979.
- (146) Lim, R. Y. H.; O'Shea, S. J. *Langmuir* **2004**, *20*, 4916.
- (147) Smith, J. A.; Werzer, O.; Webber, G. B.; Warr, G. G.; Atkin, R. *J. Phys. Chem. Lett.* **2009**, *accepted*.
- (148) Ueno, K.; Imaizumi, S.; Hata, K.; Watanabe, M. *Langmuir* **2009**, *25*, 825.
- (149) Gelesky, M. A.; Umpierre, A. P.; Machado, G.; Correia, R. R. B.; Magno, W. C.; Morais, J.; Ebeling, G.; Dupont, J. *J. Am. Chem. Soc.* **2005**, *127*, 4588.
- (150) Torimoto, T.; Okazaki, K.; Kiyama, T.; Hirahara, K.; Tanaka, N.; Kuwabata, S. *Appl. Phys. Lett.* **2006**, *89*, 243117.
- (151) Fukushima, T.; Kosaka, A.; Ishimura, Y.; Yamamoto, T.; Takigawa, T.; Ishii, N.; Aida, T. *Science* **2003**, *300*, 2072.
- (152) Wojtkow, W.; Treciak, A. M.; Choukroun, R.; Pellegatta, J. L. *J. Mol. Catal. A: Chem.* **2004**, *224*, 81.
- (153) Mehnert, C. P. *Chemistry - A European Journal* **2004**, *11*, 50.
- (154) Mehnert, C. P.; Cook, R. A.; Dispenziere, N. C.; Afeworki, M. *J. Am. Chem. Soc.* **2002**, *124*, 12932.
- (155) Marquet, P.; Andersson, G.; Kloo, L.; Atkin, R. *in prep.* **2009**.
- (156) Yamanaka, N.; Kawano, R.; Kubo, W.; Kitamura, T.; Wada, Y.; Watanabe, M.; Yanagida, S. *Chem. Commun.* **2005**, 740.
- (157) Yamanaka, N.; Kawano, R.; Kubo, W.; Maski, N.; Kitamura, T.; Wada, Y.; Watanabe, M.; Yanagida, S. *J. Phys. Chem. B* **2007**, *111*, 4763.
- (158) Minami, I. *Molecules* **2009**, *14*, 2286.
- (159) Kamimura, H.; Kubo, T.; Minami, I.; Mori, S. *Tribol. Int.* **2007**, *40*, 620.
- (160) Kamimura, H.; Chiba, T.; Watanabe, N.; Kubo, T.; Nanao, H.; Minami, I.; Mori, S. *Tribol. Online* **2006**, *1*, 40.
- (161) Bowden, F. P.; Tabor, D. *The Friction and Lubrication of Solids*; Oxford University Press: Oxford, UK, 2001.
- (162) Pandey, S. *Analytical Chimica Acta* **2006**, *556*, 38.
- (163) Armstrong, D. W.; He, L.; Liu, Y.-S. *Anal. Chem.* **1999**, *71*, 3873.
- (164) Hardacre, C.; Holbrey, J. D.; Nieuwenhuyzen, M.; Youngs, T. G. A. *Acc. Chem. Res.* **2007**, *40*, 1146.

- (165) Deetlefs, M.; Hardacre, C.; Nieuwenhuyzen, M.; Sheppard, O.; Soper, A. K. *J. Phys. Chem. B* **2005**, *109*, 1593.
- (166) Youngs, T. G. A.; Holbrey, J. D.; Deetlefs, M.; Nieuwenhuyzen, M.; Gomes, M. F. C.; Hardacre, C. *ChemPhysChem* **2006**, *7*, 2279.
- (167) Han, X.; Armstrong, D. W. *Acc. Chem. Res.* **2007**, *40*, 1079.
- (168) Stalcup, A. M.; Cabovska, B. *J. Liq. Chromatogr. Rel. Tech.* **2004**, *27*, 1443.
- (169) He, L. J.; Zhang, W. Z.; Zhao, X.; Liu, X.; Jiang, S. X. *J. Chromatogr. A* **2003**, *1007*, 39.
- (170) Visser, A. E.; Swatloski, R. P.; Reichert, W. M.; Mayton, R.; Sheff, S.; Wierzbicki, A.; Davis, J., J.D.; Rogers, R. D. *Chem. Commun.* **2001**, 135.
- (171) Liu, Y.; Zhang, Y.; Wu, G.; Hu, J. *J. Am. Chem. Soc.* **2006**, *128*, 7456.
- (172) Bovio, S.; Podesta, A.; Lenardi, C.; Milani, P. *J. Phys. Chem. B* **2009**, *113*, 6600.
- (173) Hamilton, W. A.; Porcar, L.; Butler, P. D.; Warr, G. G. *J. Chem. Phys.* **2002**, *116*, 8533.
- (174) El Abedin, S. Z.; Saad, A. Y.; Farag, H. K.; Borisenkoa, N.; Liua, Q. X.; Endres, F. *Electrochimica Acta* **2007**, *52*, 2746.